IEEE Photonics Journal
An IEEE Photonics Society Publication

Open Access

Observation of Backward Guided-Acoustic-Wave Brillouin Scattering in Optical Fibers Using Pump–Probe Technique

Volume 8, Number 3, June 2016

Neisei Hayashi
Heeyoung Lee
Yosuke Mizuno, Member, IEEE
Kentaro Nakamura, Member, IEEE

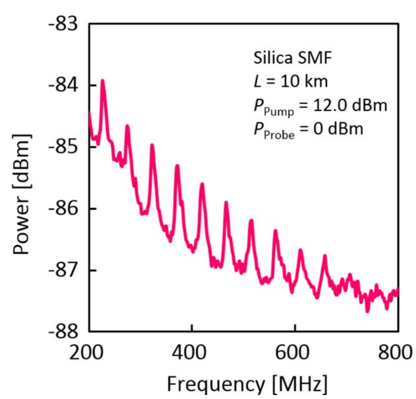

DOI: 10.1109/JPHOT.2016.2550321

Observation of Backward Guided-Acoustic-Wave Brillouin Scattering in Optical Fibers Using Pump–Probe Technique

Neisei Hayashi,[1] Heeyoung Lee,[2] Yosuke Mizuno,[2] *Member, IEEE*, and Kentaro Nakamura,[2] *Member, IEEE*

[1]Research Center for Advanced Science and Technology, University of Tokyo, Tokyo 153-8904, Japan
[2]Laboratory for Future Interdisciplinary Research of Science and Technology, Tokyo Institute of Technology, Yokohama 226-8503, Japan

DOI: 10.1109/JPHOT.2016.2550321

Manuscript received March 21, 2016; revised March 28, 2016; accepted March 29, 2016. Date of current version April 26, 2016. This work was supported in part by the Japan Society for the Promotion of Science under KAKENHI Grant 25709032, KAKENHI Grant 26630180, and KAKENHI Grant 25007652 and in part by research grants from the Iwatani Naoji Foundation, the SCAT Foundation, and the Konica Minolta Science and Technology Foundation. Corresponding author: N. Hayashi (e-mail: hayashi@cntp.t.u-tokyo.ac.jp).

Abstract: We experimentally demonstrate the observation of backward (i.e., opposite of the direction of the pump) guided-acoustic-wave Brillouin scattering (GAWBS) using the pump–probe technique and investigate the spectral dependence on the pump–probe light power. We show that the signal-to-noise ratio (SNR) of the backward GAWBS measurement can be drastically improved by using this technique. We also observe a nonmonotonic dependence of the SNR on the probe power, which indicates that optimal probe power exists for implementing GAWBS-based distributed sensors.

Index Terms: Guided-acoustic-wave Brillouin scattering (GAWBS), optical fiber sensors, nonlinear optics, pump-probe technique.

1. Introduction

Brillouin scattering in optical fibers, which is caused by the interaction between photons and acoustic phonons, can be categorized into two varieties: 1) standard Brillouin scattering, in which incident light interacts with longitudinal acoustic waves; and 2) guided-acoustic-wave Brillouin scattering (GAWBS) [1] (also referred to as forward Brillouin scattering [2], cladding Brillouin scattering [3], and transverse stimulated Brillouin scattering [4]), in which incident light interacts with transverse acoustic waves. In standard Brillouin scattering, the scattered light propagates backward (i.e., opposite to the direction of the pump) accompanying the Brillouin frequency shift (BFS), which is on the order of gigahertz (although several higher order peaks sometimes appear). On the other hand, during GAWBS, the scattered light propagates forward with multiple frequency shifts [which we refer to as guided-acoustic-wave Brillouin frequency shifts (GAW-BFSs)]; these are lower than 1 GHz and correspond to the resonance modes.

To date, standard longitudinal Brillouin scattering in optical fibers has been extensively exploited in order to develop various optical devices and systems, including not only lasers [5], slow light generators [6], optical comb generators [7], and all-optical logic gates [8], but distributed strain and temperature sensors as well [9]–[18]. However, no report has been provided on GAWBS-based distributed measurements, despite the fact that the GAW-BFS exhibits strain and temperature dependencies in the same manner that the standard BFS does [19], [20]. By using GAWBS, several physical parameters—such as the fiber outer diameter [21] and the acoustic impedances of the surrounding materials—can be additionally measured in a distributed manner. Thus, in order to fill this lacuna in the literature, in this study, we aim to achieve GAWBS-based distributed sensing.

Some distributed sensing techniques have been developed for systems based on standard Brillouin scattering, including time-domain [9]–[14] and correlation-domain techniques [15]–[18]. In the effort to directly apply these techniques to GAWBS-based systems, problems arise as a result of the mismatch between the scattering direction required by these techniques and that provided by GAWBS. More specifically, all the previously developed techniques exploit the optical path difference of the scattered light beams, and the scattered light needs to propagate backward (otherwise, the optical path difference will not occur). However, GAWBS typically generates forward-scattered light, which cannot be directly used to develop such distributed sensing systems. Therefore, successful observation of backward GAWBS light (which we define as the GAWBS light propagating in the direction opposite to the incident light) is extremely crucial to the task of integrating these various distributed sensing techniques into GAWBS-based systems.

One method of observing backward GAWBS light is to exploit stimulated Brillouin scattering (SBS), which is a phenomenon whereby the longitudinal Brillouin scattering become significantly enhanced via electrostriction when the power of the incident pump light is higher than a certain threshold. Tanaka *et al.* [22] and Dossou *et al.* [23] have reported the backward observation of GAWBS light, which consists of two components: the SBS-backscattered GAWBS light induced by the high-power pump light, and the GAWBS light induced by the SBS-backscattered high-power pump light. As the optical paths of the two components are the same, the two components need not be separated in order to develop GAWBS-based distributed sensors.

In practical applications of standard Brillouin sensors, the so-called pump-probe technique is often employed in order to improve the signal-to-noise ratio (SNR) of the measurement [24]–[26]. According to this technique, probe light and pump light are injected into opposite ends of the fiber under test (FUT). Using this technique, SBS can be induced at a much lower threshold power, leading to a higher-power Brillouin-scattered signal under the same incident pump power. Although the pump-probe technique also appears to be effective at improving the SNR of the backward GAWBS measurement, there have been no detailed reports of this phenomenon.

In this paper, we employ the pump-probe technique to observe backward GAWBS light, and investigate its spectral dependencies on the pump and probe light powers. We experimentally demonstrate that the pump-probe technique is effective at improving the SNR. More specifically, we show that the SNR dependence on the probe power is non-monotonic, which indicates the existence of an optimal probe power to be used in implementing actual GAWBS-based distributed sensors.

2. Principle of GAWBS

GAWBS, which is typically a forward scattering phenomenon, results from the interaction between incident light and the transverse modes of acoustic waves excited by small thermally induced vibrations of glass molecules [1]. The refractive index of the fiber is perturbed by the acoustic modes, leading to phase or polarization modulation in the scattering process. The GAW-BFSs are given by the resonance frequencies of the acoustic modes, which are mainly determined by the acoustic velocity (including longitudinal and transverse acoustic waves) and the fiber outer diameter. The transverse acoustic modes that cause GAWBS can be classified into two varieties [1]: radial $R_{0,m}$ modes and mixed torsional-radial $TR_{2,m}$ modes, where m is the order of the resonance. The $R_{0,m}$ modes have symmetric axes, whereas the $TR_{2,m}$ modes have symmetric planes along the optical fiber. The $R_{0,m}$ modes perturb the refractive index radially and maintain the polarization of the scattered light (referred to as polarized GAWBS). In contrast, the $TR_{2,m}$ modes perturb the birefringence and modulate the polarization of the scattered light (referred to as depolarized GAWBS). The GAW-BFS of the m-th acoustic mode $\nu_{GB,m}$ is given by [1]

$$\nu_{GB,m} = \frac{v y_m}{\pi d} \tag{1}$$

where d is the fiber outer diameter, v is the velocity of the longitudinal acoustic wave v_L (for polarized GAWBS) or transverse acoustic wave v_s (for depolarized GAWBS), and y_m is the value derived from the following equation [1]:

$$\begin{vmatrix} \left(3 - \frac{y_m^2}{2}\right) J_2(\alpha y_m), & \left(6 - \frac{y_m^2}{2}\right) J_2(y_m) - 3 y_m J_3(y_m) \\ J_2(\alpha y_m) - \alpha y_m J_3(\alpha y_m), & \left(2 - \frac{y_m^2}{2}\right) J_2(y_m) + y_m J_3(y_m) \end{vmatrix} = 0 \tag{2}$$

where $\alpha = v_s/v_L$ and J_2 and J_3 are the second- and third-order Bessel functions. The spectral powers of the $TR_{2,m}$ modes are reported to be higher than those of the $R_{0,m}$ modes [1].

The GAW-BFSs of the $TR_{2,m}$ modes are known to show strain and temperature dependencies; for instance, when m is 5, the GAW-BFS linearly depends on the strain and temperature with coefficients of ~1.9 MHz/% (at 1319 nm) [19] and ~11 kHz/K (at 1550 nm) [20], respectively. The linewidths of the GAWBS spectral peaks are also reported to strongly depend on the acoustic properties (acoustic impedance, etc.) of the material attached to the optical fiber [19], [27]. For instance, the linewidth of the GAWBS peak ($TR_{2,5}$ mode) observed using a bare fiber is ~0.3 MHz, which increases to ~4 MHz when the fiber is attached to a polymer. This behavior may be applicable to the acoustic impedance measurement of the attached materials.

The observation of the backward GAWBS signal has been performed by injecting high-power pump light [3], [22], [23]. If the pump power becomes higher than the SBS threshold, we can observe part of the GAWBS signal in the backward direction. The backward GAWBS signal involves two components. One is the GAWBS light that first propagates forward as a result of the high-power pump light and is then backscattered by the SBS process; the other is the GAWBS light that is induced by the SBS-backscattered high-power pump light. One useful technique to reduce the SBS threshold is the pump-probe technique [24]–[26], in which probe light is additionally injected into the FUT from the other end. By setting the probe frequency to $\nu_0 - \nu_B$ (ν_0: pump frequency, ν_B: BFS of the FUT), the energy transfer from pump to probe can be drastically accelerated.

3. Experimental Setup

The experimental setup for observing backward GAWBS light using the pump-probe technique is depicted in Fig. 1. A 10 km long silica single-mode fiber (SMF) with a BFS of 10.86 GHz was used as the FUT. The laser output at 1550 nm, which had a power of 6.0 dBm and a linewidth of ~1 MHz, was divided into two components using a 3 dB coupler. One light beam was used as pump light, which was polarization-controlled, amplified using an erbium-doped fiber amplifier (EDFA), and injected into the FUT. The pump light, which was transmitted through the FUT, was guided to the air via an optical circulator in order to prevent it from being reflected and injected again into the FUT. The other light beam was used as probe light, which was frequency-downshifted by the BFS of the FUT (= 10.86 GHz) using a single-sideband modulator (SSBM; the carrier suppression ratio was > 20 dB), amplified using another EDFA, and injected into the FUT from the other end. The GAWBS light propagating backward was polarized and guided to a photo detector (PD) along with the transmitted probe light. Using the PD, the beat signal between the GAWBS light and the transmitted probe light was converted into an electrical signal, which was observed using an electrical spectrum analyzer (ESA). The polarization state was

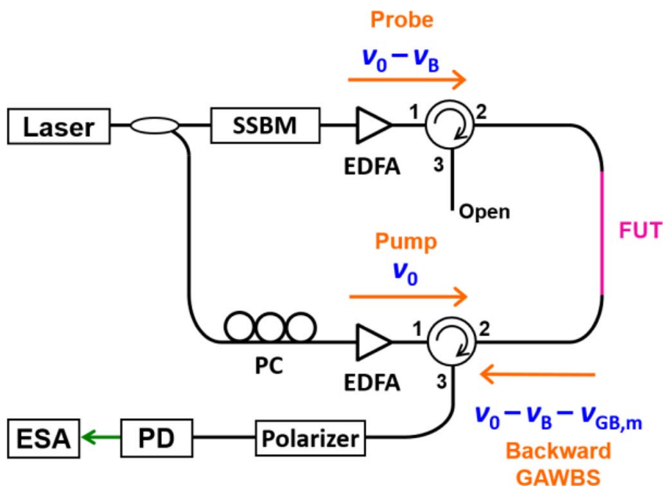

Fig. 1. Experimental setup for observing the backward GAWBS light using the pump–probe technique (EDFA: erbium-doped fiber amplifier; ESA: electrical spectrum analyzer; FUT: fiber under test; PC: polarization controller; PD: photodetector; SSBM: single-sideband modulator).

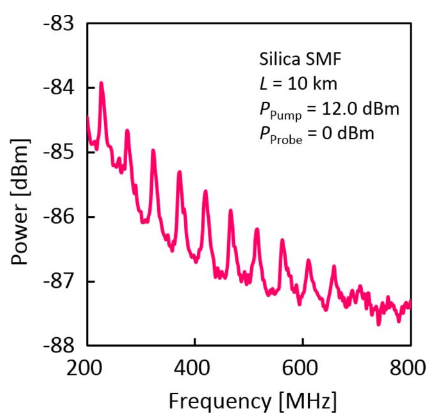

Fig. 2. Wide-range view of the observed GAWBS spectrum.

adjusted using a polarization controller (PC) so that the observed GAWBS signal was maximal. The ambient temperature was 26 °C.

4. Experimental Results

Fig. 2 shows the backward GAWBS spectrum observed for a pump power of 12.0 dBm and a probe power of 0 dBm. Approximately 10 clear peaks appeared in the frequency range from 200 MHz to 800 MHz. The GAW-BFS values of each peak agreed well with the theoretical values of each $TR_{2,m}$ mode [1].

Subsequently, we measured the pump power dependence of the GAWBS spectrum near the peak at ~320 MHz (corresponding to the $TR_{2,18}$ mode, which exhibits one of the clearest peaks). The probe power was 0 dBm. As the pump power increased, the spectral peak power increased, but the noise floor also increased [see Fig. 3(a)]. Therefore, here we define the SNR as the ratio between the spectral peak power and the spectral power at 340 MHz. Fig. 3(b) shows the pump power dependence of the GAWBS spectrum, which was normalized so that the spectral power at 340 MHz was 0 dB. The spectrum at the pump power of 3.6 dBm (regarded as the noise floor of the ESA) was subtracted from all the spectra. The SNR increased

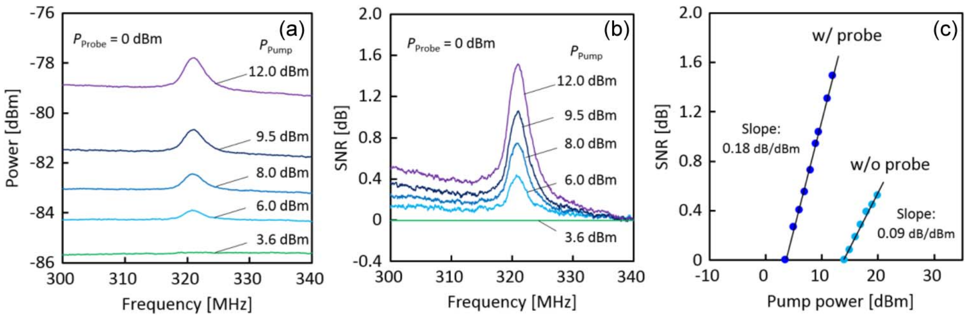

Fig. 3. (a) Pump power dependence of the GAWBS spectrum around 320 MHz. (b) Pump power dependence of the GAWBS spectrum normalized in order for the spectral power at 340 MHz to be 0 dB. (c) Pump power dependence of the SNR of the backward GAWBS measurement with and without the probe light.

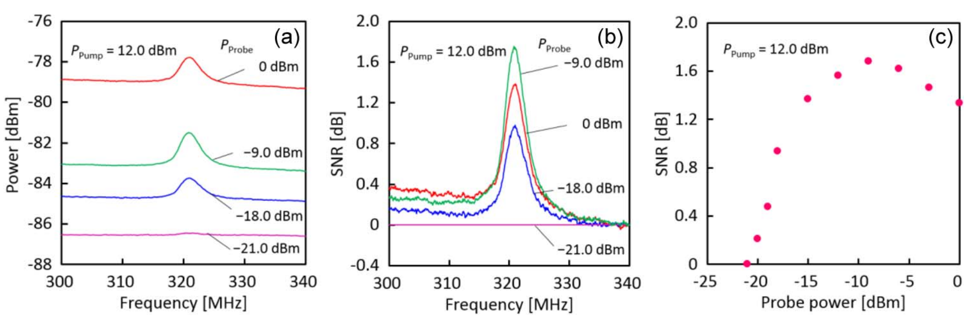

Fig. 4. (a) Probe power dependence of the GAWBS spectrum around 320 MHz. (b) Probe power dependence of the GAWBS spectrum normalized in order for the spectral power at 340 MHz to be 0 dB. (c) Probe power dependence of the SNR of the backward GAWBS measurement for a pump power of 12 dBm.

as the pump power increased. The SNR was then plotted as a function of the pump power, as shown in Fig. 3(c), which also shows the results obtained when the probe light was not injected. The backward GAWBS became observable at a pump power of 3.6 dBm, which was ~10 dB lower than the value observed without using the probe light. The SNR increased linearly as the pump power increased with a slope of 0.18 dB/dBm, which was almost twice as large as the value obtained without using the probe light. This result clearly showcases the effectiveness of the pump-probe technique in improving the SNR of the backward GAWBS measurement.

Finally, we measured the probe power dependence of the GAWBS spectrum at ~320 MHz. The pump power was 12.0 dBm. As shown in Fig. 4(a), as the probe power increased, the spectral peak power as well as the noise floor increased. The probe power dependence of the GAWBS spectrum normalized using the spectral power at 340 MHz is shown in Fig. 4(b). The spectrum at the probe power of −21.0 dBm was subtracted from all the spectra in order to suppress the influence of the noise of the ESA. Interestingly, the SNR obtained at a probe power of −9.0 dBm was higher than that obtained at 0 dBm. The SNR dependence on the probe power is shown in Fig. 4(c). The backward GAWBS signal became observable at a probe power of approximately −21 dBm. As the probe power increased up to −9.0 dBm, the SNR monotonically increased. However, as the probe power further increased above −9.0 dBm, the SNR decreased. This behavior can be explained by the fact that the increase in the noise floor (the influence of the noise caused by the ESA was negligible in this measurement) was more significant than the increase in the GAWBS signal. Note that this noise floor is actually the foot of the beat signal between the probe light and the SBS light; the power of the SBS light is much higher than that of the GAWBS light. As it is infeasible in principle to suppress this noise floor while maintaining the peak power of the backward GAWBS light, such SNR deterioration is inevitable in this scheme. This result indicates that an optimal probe power exists for developing GAWBS-based sensors using the pump-probe technique.

5. Conclusion

The backward GAWBS observation was successfully performed for the first time using the pump-probe technique, and the spectral dependencies on the pump and probe powers were investigated. The SNR was experimentally shown to drastically increase as a result of using this technique. More specifically, a non-monotonic dependence of the SNR on the probe power (at a fixed pump power) suggested the existence of an optimal probe power to be used in developing GAWBS-based sensors. These results constitute the first step in the development of backward GAWBS-based distributed sensing, and will be useful in measuring quantities such as strain, temperature, fiber outer diameter, and acoustic impedance in the future.

References

[1] R. M. Shelby, M. D. Levenson, and P. W. Bayer, "Guided acoustic-wave Brillouin scattering," *Phys. Rev. B*, vol. 31, no. 8, pp. 5244–5252, Apr. 1985.
[2] R. M. Shelby, M. D. Levenson, and P. W. Bayer, "Resolved forward Brillouin scattering in optical fibers," *Phys. Rev. Lett.*, vol. 54, no. 9, pp. 939–942, Mar. 1985.
[3] I. Bongrand, A. Picozzi, and E. Picholle, "Coherent model of cladding Brillouin scattering in single-mode fibres," *IEEE Electron. Lett.*, vol. 34, no. 18, pp. 1769–1770, Sep. 1998.
[4] I. Bongrand, E. Picholle, and C. Montes, "Coupled longitudinal and transverse stimulated Brillouin scattering in single-mode optical fibers," *Eur. Phys. J. D, Atomic, Mol., Opt. Plasma Phys.*, vol. 20, no. 1, pp. 121–127, Jul. 2002.
[5] Y. Xu, D. Xiang, Z. Ou, P. Lu, and X. Bao, "Random Fabry–Pérot resonator-based sub-kHz Brillouin fiber laser to improve spectral resolution in linewidth measurement," *Opt. Lett.*, vol. 40, no. 9, pp. 1920–1923, May 2015.
[6] K. Y. Song, M. G. Herraez, and L. Thevenaz, "Observation of pulse delaying and advancement in optical fibers using stimulated Brillouin scattering," *Opt. Exp.*, vol. 13, no. 1, pp. 82–88, Jan. 2005.
[7] G. J. Cowle, D. Y. Stepanov, and Y. T. Chieng, "Brillouin/erbium fiber lasers," *J. Lightw. Technol.*, vol. 15, no. 7, pp. 1198–1204, Jul. 1997.
[8] D. Williams, X. Bao, and L. Chen, "All-optical NAND/NOT/AND/OR logic gates based on combined Brillouin gain and loss in an optical fiber," *Appl. Opt.*, vol. 52, no. 14, pp. 3404–3411, May 2013.
[9] T. Horiguchi and M. Tateda, "BOTDA-nondestructive measurement of single-mode optical fiber attenuation characteristics using Brillouin interaction: Theory," *J. Lightw. Technol.*, vol. 7, no. 8, pp. 1170–1176, Aug. 1989.
[10] J. Urricelqui, M. Sagues, and A. Loayssa, "Phasorial differential pulse-width pair technique for long-range Brillouin optical time-domain analysis sensors," *Opt. Exp.*, vol. 22, no. 14, pp. 17403–17408, Aug. 1989.
[11] Y. Dong *et al.*, "High-sensitivity distributed transverse load sensor with an elliptical-core fiber based on Brillouin dynamic gratings," *Opt. Lett.*, vol. 40, no. 21, pp. 5003–5006, Nov. 2015.
[12] Y. Dong *et al.*, "High-spatial-resolution fast BOTDA for dynamic strain measurement based on differential double-pulse and second-order sideband of modulation," *IEEE Photon. J.*, vol. 5, no. 3, Jun. 2013, Art. no. 2600407.
[13] T. Kurashima, T. Horiguchi, H. Izumita, S. Furukawa, and Y. Koyamada, "Brillouin optical-fiber time domain reflectometry," *IEICE Trans. Commun.*, vol. E76-B, no. 4, pp. 382–390, Jul. 2014.
[14] L. E. Y. Herrera, G. C. Amaral, and J. P. von der Weid, "Investigation of bend loss in single mode fibers with ultra-high-resolution photon-counting optical time domain reflectometer," *Appl. Opt.*, vol. 55, no. 5, pp. 1177–1182, Feb. 2016.
[15] K. Hotate and T. Hasegawa, "Measurement of Brillouin gain spectrum distribution along an optical fiber using a correlation-based technique—Proposal, experiment and simulation," *IEICE Trans. Electron.*, vol. E83-C, no. 3, pp. 405–412, Mar. 2000.
[16] R. K. Yamashita, W. Zou, Z. He, and K. Hotate, "Measurement range elongation based on temporal gating in Brillouin optical correlation domain distributed simultaneous sensing of strain and temperature," *IEEE Photon. Technol. Lett.*, vol. 24, no. 12, pp. 1006–1008, Apr. 2012.
[17] Y. Mizuno, W. Zou, Z. He, and K. Hotate, "Proposal of Brillouin optical correlation-domain reflectometry," *Opt. Exp.*, vol. 16, no. 16, pp. 12148–12153, Aug. 2008.
[18] N. Hayashi, Y. Mizuno, and K. Nakamura, "Distributed Brillouin sensing with centimeter-order spatial resolution in polymer optical fibers," *J. Lightw. Technol.*, vol. 32, no. 21, pp. 3397–3401, Nov. 2014.
[19] Y. Tanaka and K. Ogusu, "Tensile-strain coefficient of resonance frequency of depolarized guided acoustic-wave Brillouin scattering," *IEEE Photon. Technol. Lett.*, vol. 11, no. 7, pp. 865–867, Jul. 1999.
[20] Y. Tanaka and K. Ogusu, "Temperature coefficient of sideband frequencies produced by depolarized guided acoustic-wave Brillouin scattering," *IEEE Photon. Technol. Lett.*, vol. 10, no. 12, pp. 1769–1771, Dec. 1998.
[21] M. Ohashi, S. Naotaka, and S. Kazuyki, "Fibre diameter estimation based on guided acoustic wave Brillouin scattering," *Electron. Lett.*, vol. 28, no. 10, pp. 900–902, Feb. 1992.
[22] Y. Tanaka, H. Yoshida, and T. Kurokawa, "Guided-acoustic-wave Brillouin scattering observed backward by stimulated Brillouin scattering," *Meas. Sci. Technol.*, vol. 15, no. 8, pp. 1458–1461, Jul. 2004.

[23] M. Dossou, D. Bacquet, A. Goffin, and P. Szriftgiser, "Observation of Cladding Brillouin Scattering (CBS) modes using backscattering technique," in *Proc. Symp. IEEE/LEOS Benlux Chapter*, Enschede, The Netherlands, 2008, pp. 35–38.
[24] G. P. Agrawal, *Nonlinear Fiber Optics*. San Diego, CA, USA: Academic, 1995.
[25] N. Shibata, Y. Azuma, T. Horiguchi, and M. Tateda, "Identification of longitudinal acoustic modes guided in the core region of a single-mode optical fiber by Brillouin gain spectra measurements," *Opt. Lett.*, vol. 13, no. 7, pp. 595–597, Jul. 1988.
[26] Y. Mizuno, M. Kishi, K. Hotate, T. Ishigure, and K. Nakamura, "Observation of stimulated Brillouin scattering in polymer optical fiber with pump-probe technique," *Opt. Lett.*, vol. 36, no. 12, pp. 2378–2380, Jun. 2011.
[27] A. J. Poustie, "Bandwidth and mode intensities of guided acoustic-wave Brillouin scattering in optical fibers," *J. Opt. Soc. Amer. B*, vol. 10, no. 4, pp. 691–696, Apr. 1993.